





Signature of Planetary Mergers on Stellar Spins

Ahmed Qureshi¹, Smadar Naoz^{1,2} , and Evgenya L. Shkolnik³ ¹ Department of Physics and Astronomy, University of California, Los Angeles, Los Angeles, CA 90095, USA; ahmed.qureshi@ucla.edu, snaoz@astro.ucla.edu² Mani L. Bhaumik Institute for Theoretical Physics, Department of Physics and Astronomy, University of California, Los Angeles, Los Angeles, CA 90095, USA³ School of Earth and Space Exploration, Arizona State University, Tempe, AZ 85281, USA

Received 2018 April 14; revised 2018 July 19; accepted 2018 July 20; published 2018 August 30

Abstract

One of the predictions of high-eccentricity planetary migration is that many planets will end up plunging into their host stars. We investigate the consequence of planetary mergers on their stellar hosts' spin period. Energy and angular momentum conservation indicate that planet consumption by a star will spin up the star. We find that our proof-of-concept calculations align with the observed bifurcation in the stellar spin-period in young clusters. For example, after a Sun-like star has eaten a Jupiter-mass planet it will spin up by $\sim 60\%$ (i.e., spin period is reduced by $\sim 60\%$), causing an apparent gap in the stellar spin-period between stars that consumed a planet and those that did not. The spun-up star will later spin down due to magnetic braking, consistent with the disappearance of this bifurcation in clusters ($\gtrsim 300$ Myr). The agreement between the calculations presented here and the observed spin-period color diagram of stars in young clusters provides circumstantial evidence that planetary accretion onto their host stars is a generic feature of planetary-system evolution.

Key words: open clusters and associations: general – planetary systems – stars: rotation

1. Introduction

Recent observations showed that many short-period exoplanets are found nearly at, or even interior to, their Roche limit (see Figure 1 in Jackson et al. 2017), implying that these planets will be consumed by their host star. In the process of spiraling into a star, star–planet tidal interactions tend to spin up the star (e.g., Dobbs-Dixon et al. 2004; Jackson et al. 2008, 2009; Lanza 2010; Brown et al. 2011; Bolmont et al. 2012). Further, it was proposed that a shortage of close-in planets around fast rotators (e.g., McQuillan et al. 2013) can be attributed to the tidal merger of planets onto a star (e.g., Lanza & Shkolnik 2014; Teitler & Königl 2014).

Driving a planet on a nearly radial orbit seems to be one of the natural consequences of the eccentric Kozai–Lidov mechanism (for a recent review see Naoz 2016). In this process, a far away companion can induce large planetary orbit eccentricity and plunge it into the star (e.g., Guillochon et al. 2011; Naoz et al. 2012; Li et al. 2014; Valsecchi & Rasio 2014; Petrovich 2015a, 2015b; Rice 2015; Stephan et al. 2017, 2018). Smaller and moderate eccentricities are expected from planet–planet interactions, but may still result in many planets plunging into the star (e.g., Naoz et al. 2011; Antonini et al. 2016; Petrovich & Tremaine 2016; Hamers 2017). Here, we show that as a planet falls onto a star, it deposits its energy, angular momentum, and mass into the star, causing the star to spin up.

Stellar rotation is attributed to a combination of both stellar mass and evolutionary state. Sun-like stars spin down by losing angular momentum to magnetized stellar winds, otherwise known as magnetic braking, during the main-sequence stage (e.g., Parker 1958; Schatzman 1962; Weber & Davis 1967; Mestel 1968). Therefore, the stellar rotation-period or the rotational velocity $v_{\text{rot}} \sin i$ is frequently used as a proxy for stellar ages (e.g., Barnes 2003a, 2003b, 2007; Mamajek & Hillenbrand 2008; Meibom et al. 2009, 2011; James et al. 2010; van Saders & Pinsonneault 2013; van Saders et al. 2016).

Mamajek & Hillenbrand (2008) showed that the spin period of stars in the Pleiades open cluster (age ≈ 130 Myr) exhibits a

bifurcation for the same effective temperature ($B - V$) values. One group of stars is fast rotators (with spin-periods of 1–2 days) and another one is slower rotators (with spin-periods of 3–9 days). Mamajek & Hillenbrand (2008) showed that the latter group's spin period traces the spin-fit models adopted from Barnes (2007). This behavior is also observed in other young clusters such as M35 and M34 (100 Myr and 240 Myr, respectively; e.g., Meibom et al. 2009; James et al. 2010).⁴ Moreover, it seems that fast rotators have a dearth of close-in planets around them (e.g., McQuillan et al. 2013; Lanza & Shkolnik 2014). Observations suggest that this bifurcation is suppressed for older clusters such as the Hyades (≈ 625 Myr) and M48 (≈ 380 Myr) (Saar & Brandenburg 1999; Pizzolatto et al. 2003; Mamajek & Hillenbrand 2008; Meibom et al. 2009; Nardiello et al. 2015).

One interpretation for this division in rotation periods is that the fastest rotators have an outer convective magnetic field zone that shears the interior radiative zone and causes the gap in the rotation (e.g., Barnes 2003a, 2003b; Meibom et al. 2009; James et al. 2010). In other words, this interpretation suggests that fast rotators possess only a convective field. Thus, they are inefficient in depleting their spin angular momentum. Later, van Saders et al. (2016), using evolutionary modeling, suggested that this gap is a result of a weaker magnetic braking process. Their models were able to reproduce both the asteroseismic and the cluster data. Recently, Somers & Stassun (2017) analyzed the radii of single stars in the Pleiades and showed that inflated stars have a shorter spin period. Their statistical analysis included the inflation of young stars by magnetic activity and/or starspots. Furthermore, stellar evolution (SE) models of zero-main-sequence radii contraction were able to produce consistent results with the observations of rotation period in the star-forming regions and young open clusters (e.g., Gallet & Bouvier 2013, 2015). Recently, a new model for stellar spin-down by Garraffo et al. (2018) was suggested, taking into account the stellar surface magnetic field

⁴ See Table 1 for open cluster age estimations.

configuration as a plausible explanation for the observed bimodal spin-period distribution.

Observations of the young open clusters such as h Persei, (~ 13 Myr; e.g., Moraux et al. 2013), NGC 2264 (~ 2 Myr; e.g., Kearns et al. 1997), and NGC 2362 (~ 5 Myr; e.g., Irwin et al. 2008) give a glimpse into the birth rotational period distribution of stars. Unlike the clusters mentioned above, these extremely young clusters do not show a clear bifurcation signature, but instead a nearly uniform distribution. For slightly older clusters ($\gtrsim 100$ Myr) a clear split between fast and slow rotators emerges, with the slow rotators' spin-periods fitting the magnetic braking SE model (see below, Section 2.1 and Figure 2). For much older clusters ($\gtrsim 400$ Myr) the bifurcation disappears. The question then is, what is the underlining mechanism that produces or maintains only the fast rotator population for a period of few hundreds of million years. The aforementioned magnetic models might be at play.

Here, we offer an alternative scenario: an increase in stellar rotation of a star due to the consumption of a Jupiter-mass planet. A planet may plunge into the star, for example, due to high-eccentricity migration. Thus, the star will absorb both the mass of the planet and the planet's orbital angular momentum, and will cause the star to spin up.

In this model, the young clusters represent the birth population, before giant planets formed (since they are typically expected to take place on a few to ~ 10 Myr; e.g., Pollack et al. 1996). Subsequently, magnetic braking will drive the stars to slow down. As dynamical processes take place on the order of ~ 10 – 100 Myr, stars consume planets and thus spin up.

We note that the detailed process at which a planet accretes onto the star is complicated (e.g., Metzger et al. 2012, 2017; Pejcha et al. 2016; Dosopoulou et al. 2017; Ginzburg & Sari 2017). However, our calculations are independent of the process and depend only on the result because we consider angular momentum conservation, associated with the merger. We compare our calculations with several observed open cluster period–color diagrams and show that a planet consumed by a star at about 100 Myr fits the observations.

The paper is organized as follow. We begin with considering the effects on the stellar spins (Section 2). In particular, we consider magnetic braking (Section 2.1), angular momentum conservation (Section 2.2), and energy arguments (Section 2.3). We then continue with a description of the consequences of consumption of a planet on the stellar spin-period (Section 3). We finally offer our discussion in Section 4.

2. Effects on the Stellar Spin

2.1. Magnetic Braking

As mentioned, Sun-like stars undergo spin-down due to magnetic braking (e.g., Parker 1958; Schatzman 1962; Weber & Davis 1967; Mestel 1968). The spin-loss rate is evaluated as

$$\dot{\Omega} = -\alpha_{\text{mb}} \Omega^2, \quad (1)$$

(e.g., Dobbs-Dixon et al. 2004), where

$$\alpha_{\text{mb}} = \begin{cases} 1.5 \times 10^{-14} \text{ years} & \text{G stars} \\ 1.5 \times 10^{-15} \text{ years} & \text{F stars.} \end{cases} \quad (2)$$

We use the single-star evolution (SSE) code (e.g., Hurley et al. 2000) with the magnetic braking from Equation (1) to calculate the spin evolution of the stars as a function of time for stellar

masses between 0.6 and $1.8 M_{\odot}$. Note that by implementing Equation (1) in the SSE we also include the nominal dependency of the mass of the stellar envelope (e.g., Hurley et al. 2000), which results in a different time evolution. For example, the magnetic braking from Hurley et al. (2000) underestimates the spin period of a Sun-like star by a factor of 5 at ~ 5 Gyr, while the Dobbs-Dixon et al. (2004) recipe yields a closer value for the Sun's spin rate. We take the initial spins from the SSE, and they range from 10.4 days to 0.8 day for masses of 0.6 to $1.8 M_{\odot}$, respectively.

2.2. Angular Momentum Arguments

During the final step of high-eccentricity migration, when the planet plunges in, we assume angular momentum conservation. We note that during the dynamical evolution the angular momentum of the inner orbit is not necessarily conserved, as an inclined companion can exchange angular momentum with the inner planet (e.g., Naoz et al. 2011, 2013). However, during the final plunge, the inner orbit decouples from the outer orbit, and thus it can be characterized with angular momentum conservation (e.g., Naoz & Fabrycky 2014, Figure 3). The equation in this case is

$$L_i = I_s \Omega_s + I_p \Omega_p + L_{\text{orb}}, \quad (3)$$

where Ω_s (Ω_p) is the star's (planet's) spin rate; the star's and the planet's moments of inertia are $I_s = 0.08 M R^2$ and $I_p = 0.26 m r^2$, respectively (e.g., Eggleton & Kiseleva-Eggleton 2001), where R (r) is the radius of star (planet). We note that the radius of the star is assumed to stay constant post-consumption. Subscript “ i ” denotes the initial (pre-consumption) state. The magnitude of the orbital angular momentum L_{orb} for an orbit with a semimajor axis a and eccentricity e is given by

$$L_{\text{orb}} = \frac{Mm}{M+m} \sqrt{G(M+m)a(1-e^2)} \\ \approx \frac{Mm}{M+m} \sqrt{2G(M+m)R_{\text{Roche}}}, \quad (4)$$

where M and m are the masses of the star and the planet, respectively. For plausible Ω_p , the angular momentum associated with planetary spin can be neglected compared to L_{orb} and $I_s \Omega_s$. Thus, Equation (3) can be approximated as

$$L_i \approx I_s \Omega_s + L_{\text{orb}}. \quad (5)$$

In the last transition in Equation (4), we assumed high eccentricity so that $e \rightarrow 1$, and thus $a(1-e^2) \approx 2a(1-e) \approx 2R_{\text{Roche}}$, where R_{Roche} is the Roche limit given by

$$R_{\text{Roche}} \sim \eta r \left(\frac{m}{M+m} \right)^{-1/3}, \quad (6)$$

where η is a numerical parameter of the order of unity. We adopt $\eta = 1.6$ and note that changing the value of η does not qualitatively change the dynamical nature of the system but rather the efficacy of the disruption of planets (e.g., Petrovich 2015a). Angular momentum conservation yields

$$L_i = L_f, \quad (7)$$

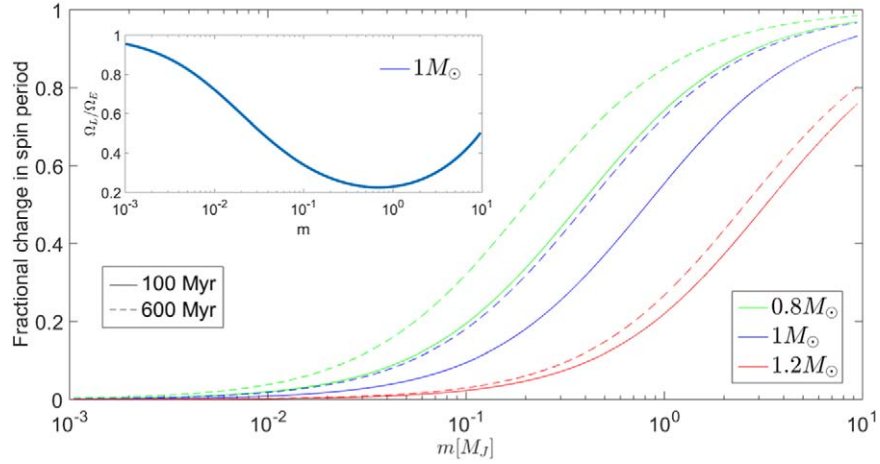


Figure 1. Spin period absolute percentage change, defined as $|P_{\Omega,i} - P_{\Omega,f}|/P_{\Omega,i}$, as a function of the planet mass. The solid lines depict a merger that took place after 100 Myr, while the dashed lines represent a merger after 600 Myr of stellar evolution. The planet was assumed to plunge in from a distance of 5 au (as noted above, the actual initial distance does not significantly change the results). We consider three representative stellar masses of 0.8, 1, and $1.2 M_{\odot}$, shown in green, blue, and red, respectively. In the inset, the ratio of the post-spin for angular momentum over conservation of energy is plotted vs. the mass of the planet in terms of M_J for $1 M_{\odot}$ for a collision at 100 Myr.

where

$$L_f = I_{s+p} \Omega_{s+p}. \quad (8)$$

In this case, the total angular momentum of the system is the star’s spin rate Ω_{s+p} , where $s+p$ denotes the final star and planet object. We solve Equation (7) for Ω_{s+p} . Note that the angular momentum of the perturber should not have changed during the high-eccentricity migration. Moreover, even if a scattering took place and a far away planet was lost from the system, the angular momentum associated with it is orders of magnitude smaller than the ones in Equation (3), and thus do not affect the above analysis. For $m \ll M$ we find that $I_s \Omega_s$ is larger or comparable to L_{orb} , and thus $\Omega_{s+p,L} \sim \text{Const}$.

As can be seen from the above equations, the key parameter in determining the final spin rate for a given star is the planet’s size. This is depicted in Figure 1, where we explore a large range of companion planets’ masses from $10^{-3} M_J$ up to $10 M_J$, where M_J is the mass of Jupiter. We adopt the following mass-radius relation for the planet:

$$\frac{m}{M_{\oplus}} = \left(\frac{r}{R_{\oplus}} \right)^{2.06} \quad (9)$$

(e.g., Lissauer et al. 2011), where subscript \oplus denotes Earth’s value. We also test a simple relation for which $m \sim 3r$ (e.g., Weiss & Marcy 2014), and we find consistent results.

In Figure 1, as a proof of concept, we initially consider three representative stellar masses, 0.8, 1, and $1.2 M_{\odot}$ (red, blue, and green lines, respectively, in Figure 1). We evolve their spin period and let each star consume a planet. We consider two merger times, one is after 100 Myr and the other is after 600 Myr. In Figure 1, we show the fractional change of the spin period, specifically, $(P_{\Omega,i} - P_{\Omega,f})/P_{\Omega,i}$. Note that $P_{\Omega,i} > P_{\Omega,f}$, and we show the absolute magnitude in the figure for illustrative purposes. As depicted in Figure 1, a more massive planet is more likely to spin up the star. For example, a Jupiter-mass planet can cause a spin up of about 70% compared to the spin pre-merger for a $1 M_{\odot}$ star. For a $1.2 M_{\odot}$, the change in spin is 20%, which is much less than the smaller mass star. On the other hand, an Earth-mass planet yields an insignificant

change to the spin period for any star from 0.8 to $1.2 M_{\odot}$ after 100 and 600 Myr. Below, we will examine a mass range between 0.6 and $1.8 M_{\odot}$.

2.3. Energy Arguments

In some cases, planets that plunge into their star may be completely consumed by their star without any heat or radiation loss for the system (unlike systems for which a dusty disk is formed, e.g., Metzger et al. 2017; or increase their luminosity due to the engulfment of a planet, e.g., Metzger et al. 2012; MacLeod et al. 2018). In this case, we can assume total energy conservation, and thus before the merger it can be written as

$$E_i \sim -\frac{GMm}{2a} - \frac{GM^2}{R} - \frac{Gm^2}{r} + \frac{1}{2}I_s \Omega_{s,i}^2 + \frac{1}{2}I_p \Omega_{p,i}^2. \quad (10)$$

Note that numerical factors at the order of unity that arise from the star’s and planet’s density profiles in internal energies are neglected from the above equation for simplicity.

Energy conservation yields that the energy after the planet has been consumed by the star can be written as

$$E_i = E_f, \quad (11)$$

where E_f is the energy post-merger, with the subscript “f” denoting the final (post-consumption) state. The final energy state can be written as

$$E_f = -\frac{G(M+m)^2}{R} + \frac{1}{2}I_{s+p} \Omega_{s+p}^2. \quad (12)$$

In this case, the total energy of the orbit consists of the potential energy and the star’s new rotational kinetic energy, which is denoted as Ω_{s+p} to indicate that it is after the star consumed the planet. We then solve for the post-merger spin period $P_{\Omega,f} = 2\pi / \Omega_{s+p}$.

As implied from Equation (10), the planet’s orbital energy is much smaller than the star’s internal energy, and thus it can be neglected. We adopt a high-eccentricity migration, which often results in near radial planetary orbits, and set the planet’s initial semimajor axis to be 5 au. However, from the mentioned orbital energy arguments, the calculation below is valid for a

Table 1
Relevant Observation Parameters for the Open Clusters Used Below

Name	Age ^a (Myr)	Metallicity [Fe/H]	Period References	Metallicity References
M35	100	−0.21	Meibom et al. (2009)	Barrado y Navascués et al. (2001)
Pleiades	130	0.03	Mamajek & Hillenbrand (2008)	Soderblom et al. (2009)
M34	240	0.07	James et al. (2010)	Schuler et al. (2003)
M48	380	0.08	Barnes et al. (2015)	Netopil et al. (2016)
Hyades	625	0.4	Mamajek & Hillenbrand (2008)	Quillen (2002)

Note.

^a Note that other age estimations exist in the literature, which we refer to below. The other age estimations do not change our results, and we discuss them in the text. The age estimate of M35 in the literature ranges from 70 to 200 Myr. Reimers & Koester (1988) used white dwarf cooling age and estimated a range between 70 and 100 Myr; later, Barrado y Navascués et al. (2001) with the same technique, found an age estimate of 180 Myr (Kalirai et al. 2003). Other estimations place M35 at about 150 Myr (e.g., Sarrazine et al. 2000; von Hippel et al. 2002; Meibom et al. 2009; Leiner et al. 2015). We note that while the age of M35 might be older than the one we adopt here, the scatter in the bifurcation is consistent with the scatter in the Pleiades. The age of Pleiades varies from 100 to 180 Myr (e.g., Belikov et al. 1998; Herbst et al. 2001; Mamajek & Hillenbrand 2008). The age of M34 is consistent with 240 Myr (e.g., James et al. 2010; Meibom et al. 2011). The age of M48 varies from 380 to 450 Myr (e.g., Barnes et al. 2015; Netopil et al. 2016). Finally, we found that age estimation of Hyades can be as high as 750 Myr (e.g., Mamajek & Hillenbrand 2008; Brandt & Huang 2015).

wide range of initial separations. We have also confirmed that our calculations are consistent with the results when setting the planet to be as close as 0.02 au. In fact, as is apparent from Equations (10) and (12) for a given stellar mass, the main parameter that affects the final stellar rotation in this scenario is the planet’s mass.

Adopting a simple mass–radius relation as before ($m \sim r^\beta$), we find that the final spin period for very small mass planets ($m \ll M$) depends on the mass of the planet, i.e.,

$$\Omega_{s+p,E} \sim m^{1-\frac{1}{2\beta}}, \quad (13)$$

where the subscript “E” stands for the energy argument. In deriving Equation (13), we assumed a high-eccentricity migration, which yields that the orbital energy is much smaller than the binding energy of the planet and the star. Moreover, for typical values of star and planet spin rotation, the rotational energy is smaller than their binding energy. Finally, we focus on the dependency of final rotation rate on the planet’s mass. However, we note that the spin rate also depends on the star’s radius and mass; since we assume that these did not change in the consumption process, we drop them in the above equation. In the inset of Figure 1, we show the relation between the resulting spin due to the energy or angular momentum conservation. As depicted in the Figure 1, Ω_L/Ω_E is almost 1 for $M_J/1000$ (M_\oplus) and reaches a minimum near the mass of Jupiter.

3. Consumption of a Planet by Its Star

We compare our model to the period distribution of stars for five open clusters that span a range of ages. Specifically, we chose (from ≈ 100 to 625 Myr): M35, Pleiades, M34, M48, and Hyades; see Table 1 for the relevant parameters. We focus on a stellar-mass range of 0.6–1.8 M_\odot . As is apparent from Figure 2, all of the young clusters appear to have a bifurcation in their period distribution. However, the old clusters do not have a fast rotating population.

As illustrated in Figure 1, the largest spin-up effect will happen if a star merges with a massive planet. We adopt a Jupiter-mass planet and explore the consequences of planet consumption on the spin period as a function of the $B - V$. For each cluster, we evolve the spin period up to the cluster age, as

explained above. As can be seen in Figure 2, the SE model agrees with the slow rotator (long period) population.⁵ We also adopt an ad hoc consumption time consistent with the youngest cluster (M34, which is ≈ 100 Myr). We calculate the spin period of the star after a merger with a Jupiter-sized planet has taken place, using angular momentum conservation, for all of clusters (dashed lines, labeled “Merger” for a spin-up). As shown in this figure, the resulting post-consumption spin period is consistent with the observed fast rotator (short spin period) stars in the young clusters (top three panels). Based on these five cluster examples, it seems that the bifurcation is eliminated by ≈ 300 Myr (roughly the age of M48).

We also show that the spin period from energy conservation arguments (see Section 2.3), labeled “EC,” agrees with the short-period stellar population in young clusters. In fact, the shortest spin-periods seem to be in a better agreement with the energy conservation arguments than with the angular momentum argument period predictions. This suggests that near radial orbits during high-eccentricity migration (e.g., Naoz 2016) are common.

It is worth noting that, for a given mass, the initial spin of a star plays an insignificant role in determining post-consumption spin, for both the energy and angular momentum approaches. While the initial spin of the star is an important factor for the magnetic braking and the SE process, the main contributor for the *post-consumption* stellar spin is the size of the planet. Thus, taking the h Persei young open cluster as a birth population, or even setting the consumption time to be 13 Myr, does not change our results. However, if consumption would have taken place after 13 Myr, then our scenario predicts a clear bifurcation signature that does not exist in h Persei (see, for example, Figure 10 in Moraux et al. 2013). Thus, motivated by observations, and consistent with theoretical arguments (e.g., Naoz et al. 2012; Stephan et al. 2017), we set the consumption time at 100 Myr, which is roughly the age of M34, where the earliest bifurcation of rotation periods is observed.

Many of the clusters are older than the consumption time, and one can expect that post-merger stars will continue spin down due to magnetic braking. This process may be different

⁵ Some of these clusters have a large range of age estimations in the literature; see Table 1. In Figure 2, we show the SE model for the maximum age estimates for these clusters.

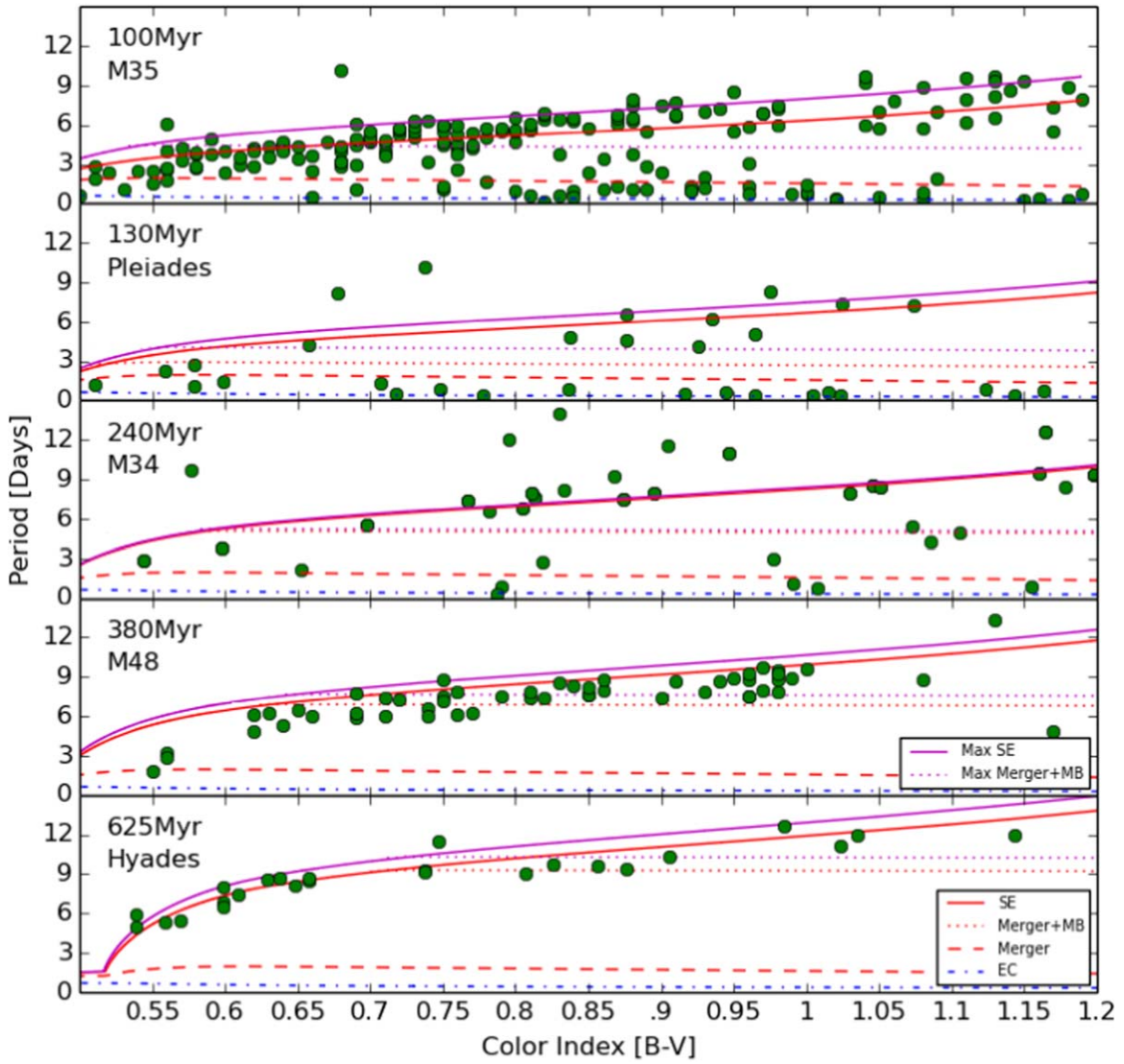


Figure 2. Spin period as a function of $B - V$. The solid red lines depict the expected period of stars for their clusters’ respective ages (labeled “SE”) following stellar evolution. The dashed lines represent the spin period post-merger at the time of the Jupiter-mass planet merger, using angular momentum arguments, labeled “Merger” (adopted to be consistent with the youngest cluster age of 100 Myr). We also consider the post-merger spin period using energy conservation arguments, labeled “EC,” blue dashed-dotted line. The dotted red line depicts the expected spin-periods that have undergone a merger at 100 Myr and subsequently went through the magnetic braking process to reach their cluster present age (labeled “Merger + MB”). We also consider the expected spin period due to stellar evolution for the maximum published age of each cluster (see Table 1), purple solid lines, labeled “Max SE.” The post-merger spin period (using angular momentum arguments), followed by magnetic braking all the way to the maximum age estimation is shown by dotted purple lines, labeled “Max Merger + MB.” The green dots are observed rotation periods of confirmed members of the above clusters adopted from Meibom et al. (2009), Mamajek & Hillenbrand (2008), James et al. (2010), and Barnes et al. (2015); see Table 1.

than the nominal magnetic braking as the new mass might not be evenly distributed, or the metallicity and magnetic field may change. Nonetheless, for simplicity, we only follow the regular magnetic braking evolution (as described above, labeled “Merger + MB”) and caution that this treatment is incomplete, as it does not include the SE complexities that SSE considers. This estimation should only be used as an order of magnitude approximation. The result is shown as a dashed-dotted line in Figure 2 and can be seen to perhaps match the scatter in those plots.

We note that the SE is calculated in terms of the effective temperature. We then convert the theoretical effective temperature to $B - V$ colors following the Sekiguchi & Fukugita (2000) fit equation. This fit depends on the metallicity of the cluster.

As shown in Figure 2, a Jupiter-mass planet accreting onto a star at early times (≈ 100 Myr) is consistent with spin-up of these stars. As the cluster grows old, the star spins down and approaches the nominal SE time.

As mentioned above, some of these open clusters have a range of published ages (see Table 1). In Figure 2, we also consider the maximum age estimation and show that our models are consistent with the observed scatter in the spin period. In particular, we show the spin period as a result of the SE model for its maximum age estimate (purple lines, labeled “Max SE”). We also calculate the spin-down of a star post-planet-consumption, using angular momentum conservation (purple dotted line, labeled “Max Merger + MB”), which also agrees with the observed cluster. Thus, we conclude that the range of age estimation does not alter our results.

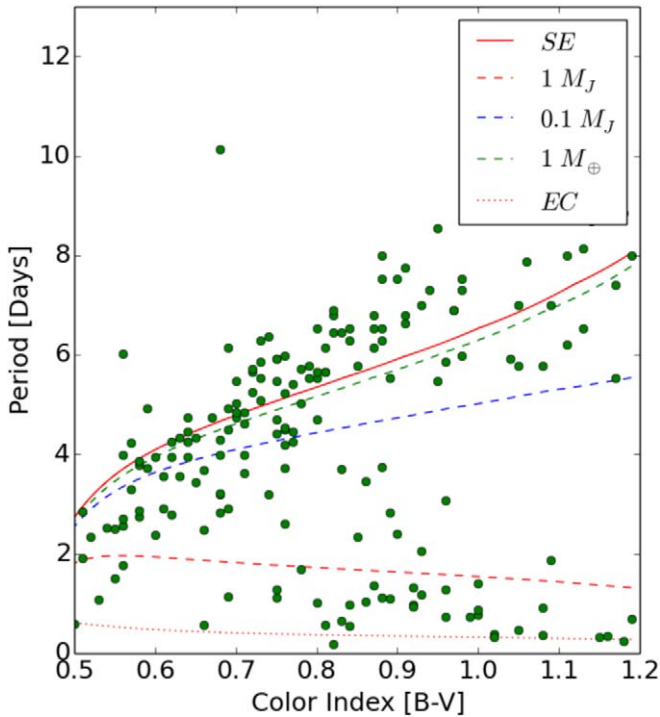


Figure 3. Spin period as a function of the $B - V$ values for the M35 open cluster. The solid line depicts the expected spin period as a result of magnetic braking spin evolution after 100 Myr, while the dashed lines represent the spin period post-merger of a planet with a mass of M_J , $M_J/10$ and M_\oplus (from bottom to top). The dotted line represents a merger of $1 M_J$ mass planet based on energy conservation (EC).

We also speculate that accretion of various planetary masses may account for the scatter in the spin period observed for young clusters. This is illustrated in Figure 3, where we calculated the post-merger spin period of a star after the consumption of a planet with a mass of M_J , $M_J/10$ and an Earth-mass (M_\oplus) planet. As depicted in Figure 3, the scatter in the young cluster is consistent with the accretion of various planetary masses.

4. Discussion

We presented a proof-of-concept calculation that shows that the observed spin-period bifurcation in young clusters is consistent with stars that consumed a planet. We considered angular momentum conservation arguments and showed that consumption of a planet can significantly spin up the star (lowering the spin period). Energy conservation arguments (where a planet is being plunged almost radially into the star) give consistent results. Both angular momentum and energy arguments yield a faster rotation after a consumption of a massive planet, such as a Jupiter-mass one.

One of the predictions from high-eccentricity migration is that planets will end up consumed by their parent star in the range of 10–100 Myr (e.g., Rasio & Ford 1996; Chatterjee et al. 2008; Guillochon et al. 2011; Naoz et al. 2012; Li et al. 2014; Valsecchi & Rasio 2014; Petrovich 2015a, 2015b; Rice 2015; Stephan et al. 2017). In some cases, the perturber can yield a plunging time that can go up to 1 Gyr (e.g., Anderson et al. 2016). Observationally, many giant planets seem to exist on decaying orbits, or on orbits that are interior to their Roche limit (Jackson et al. 2017, Figure 1), consistent with high-eccentricity migration. Thus, planets plunging into a star may be a generic feature of planetary evolution. While the details of

a planet accreting onto a star may be complicated (i.e., either disrupting and forming a disk or simply colliding; Dosopoulou et al. 2017), our calculations focus only on the consequences of planet consumption, and hence we used energy and angular momentum conservation arguments that are independent of the details of the merger process.

We calculated the effects of a planetary merger on the host stellar spin, using magnetic braking and angular and energy conservation arguments. We adopted an ad hoc consumption time consistent with the youngest cluster (≈ 100 Myr). The planet’s orbital angular momentum is absorbed by the star, causing the star to spin up. Similarly, energy conservation arguments yield that the planet’s binding energy is being absorbed by the star, causing the star to spin up. We note that during the planet consumption process energy might not be conserved (e.g., Metzger et al. 2017), but angular momentum should be conserved.⁶ Note that some planets may plunge directly into their host star, consistent with minimum energy loss. The consumption of a more massive planet (i.e., Jupiter-mass) will cause a more significant spin-up (as depicted in Figure 1).

We compared our calculations with the observed spin period of stars in five open clusters. We find that the observed stellar rotation-period bifurcation in young clusters is consistent with the spin-up due to a merger of a Jupiter-mass planet (see Figure 2). The agreement of our calculations with observations suggests that dynamical planetary accretion onto their host stars is a common characteristic in high-eccentricity planetary-system evolution (as predicted by theoretical models; e.g., Guillochon et al. 2011; Naoz et al. 2011, 2012; Li et al. 2014; Valsecchi & Rasio 2014; Muñoz & Lai 2015; Petrovich 2015a, 2015b; Rice 2015; Storch & Lai 2015; Stephan et al. 2017).

The observations presented in Figure 2 show a reduction in the bifurcation strength with time. In other words, as the cluster ages, there are fewer fast rotators. Motivated by the observations, we adopted a merger time of 100 Myr, which is the youngest cluster considered. Interestingly, this merger time is also approximately consistent with the expected merger time from high-eccentricity migration simulations (e.g., Stephan et al. 2017).

Note that it was also suggested that disk migration will, in some cases, result in plunging Earth- and super-Earth-type planets onto their host stars (e.g., Batygin & Laughlin 2015).⁷ The consumption of these planets yields a smaller change in the spin period of stars (as shown in Figures 1 and 3). On the other hand, consumption of smaller planets, or different consumption times, may account for some of the observed scatter in a fast rotator’s typical spin-period value (as depicted in Figure 2). We can also estimate the efficiency with which our mechanism is producing fast rotators. We note that the number below is highly uncertain and should only be considered at the order of magnitude level. The fraction of stars that will consume a planet is defined as

$$f = f_b f_p f_{\text{merge}}, \quad (14)$$

where f_b is the fraction of stars in binary systems, f_p is the fraction of stars with planets that may undergo high-eccentricity migration, and finally, f_{merge} is the fraction of

⁶ Note that the angular momentum that is carried out by the planet mass loss during the merger is significantly smaller than the orbital angular momentum.

⁷ High-eccentricity migration can also result in plunging Earth-size planets onto their host star (Rice 2015).

planets that merged for a specific high-eccentricity migration. We estimate $f_b \sim 0.5$ (e.g., Raghavan et al. 2010), though this is an underestimation since planets can also cause planets to merge with their host stars (e.g., Naoz et al. 2011; Petrovich 2015b). The occurrences of planets are estimated roughly as $f_p \sim 0.1$ – 0.9 . Jupiter-mass planets formed from one to few au from their star (e.g., Cumming et al. 2008; Wright et al. 2012; Bowler 2016) up to $f_p \sim 1$ for Neptune-mass planets (the solar system, for example, has two, Uranus and Neptune). Finally, the merger fraction is estimated as between $f_{\text{merger}} \sim 0.15$ and 0.25 depending on the parameters of the system and is roughly independent of the mass of the planet (e.g., Naoz et al. 2012; Petrovich 2015a; Anderson et al. 2016; Stephan et al. 2017). This gives $f \sim 0.013$ – 0.13 . The fraction of fast rotators in the cluster population is estimated from the presented data as about 30%. This implies that about 4%–42% of all fast rotators can plausibly result from the process of feeding on their planets. The fraction may increase significantly if we consider the full range of planetary masses and the full high-eccentricity migration scenarios (for example, allowing for a range of companions, such as planets).

If, indeed, the primary driver for plunging Jupiter-size planets into a star is high-eccentricity migration, then the calculation presented here suggests that the fast rotators are more likely to have a far away companion (either a star, a planet, or a brown dwarf; e.g., Rasio & Ford 1996; Naoz et al. 2011, 2012; Tutukov & Fedorova 2012; Petrovich 2015b, 2015a; Anderson et al. 2016; Stephan et al. 2017). This prediction may help disentangle the scenario suggested here and the magnetic origin for the fast rotators.

We thank the referee for useful and thoughtful comments. We also thank Alexander Stephan, Jennifer van Saders, Eric Mamajek, and Brad Hansen for useful discussions. S.N. acknowledges the partial support of the Sloan fellowship and also the partial support from the NSF through grant No. AST-173916. E.S. appreciates support from the NASA Origins of Solar System grant NNX13AH79G/80NSSC18K0003.

ORCID iDs

Smadar Naoz  <https://orcid.org/0000-0002-9802-9279>

Evgenya L. Shkolnik  <https://orcid.org/0000-0002-7260-5821>

References

- Anderson, K. R., Storch, N. I., & Lai, D. 2016, *MNRAS*, **456**, 3671
- Antonini, F., Hamers, A. S., & Lithwick, Y. 2016, *AJ*, **152**, 174
- Barnes, S. A. 2003a, *ApJL*, **586**, L145
- Barnes, S. A. 2003b, *ApJ*, **586**, 464
- Barnes, S. A. 2007, *ApJ*, **669**, 1167
- Barnes, S. A., Weingrill, J., Granzer, T., Spada, F., & Strassmeier, K. G. 2015, *A&A*, **583**, A73
- Barrado y Navascués, D., Deliyannis, C. P., & Stauffer, J. R. 2001, *ApJ*, **549**, 452
- Batygin, K., & Laughlin, G. 2015, *PNAS*, **112**, 4214
- Belikov, A. N., Hirte, S., Meusinger, H., Piskunov, A. E., & Schilbach, E. 1998, *A&A*, **332**, 575
- Bolmont, E., Raymond, S. N., Leconte, J., & Matt, S. P. 2012, *A&A*, **544**, A124
- Bowler, B. P. 2016, *PASP*, **128**, 102001
- Brandt, T. D., & Huang, C. X. 2015, *ApJ*, **807**, 58
- Brown, D. J. A., Collier Cameron, A., Hall, C., Hebb, L., & Smalley, B. 2011, *MNRAS*, **415**, 605
- Chatterjee, S., Ford, E. B., Matsumura, S., & Rasio, F. A. 2008, *ApJ*, **686**, 580
- Cumming, A., Butler, R. P., Marcy, G. W., et al. 2008, *PASP*, **120**, 531
- Dobbs-Dixon, I., Lin, D. N. C., & Mardling, R. A. 2004, *ApJ*, **610**, 464
- Dosopoulou, F., Naoz, S., & Kalogera, V. 2017, *ApJ*, **844**, 12
- Eggleton, P. P., & Kiseleva-Eggleton, L. 2001, *ApJ*, **562**, 1012
- Gallet, F., & Bouvier, J. 2013, *A&A*, **556**, A36
- Gallet, F., & Bouvier, J. 2015, *A&A*, **577**, A98
- Garraffo, C., Drake, J. J., Dotter, A., et al. 2018, *ApJ*, **862**, 90
- Ginzburg, S., & Sari, R. 2017, *MNRAS*, **469**, 278
- Guillochon, J., Ramirez-Ruiz, E., & Lin, D. 2011, *ApJ*, **732**, 74
- Hamers, A. S. 2017, *MNRAS*, **466**, 4107
- Herbst, W., Bailer-Jones, C. A. L., & Mundt, R. 2001, *ApJL*, **554**, L197
- Hurley, J. R., Pols, O. R., & Tout, C. A. 2000, *MNRAS*, **315**, 543
- Irwin, J., Hodgkin, S., Aigrain, S., et al. 2008, *MNRAS*, **384**, 675
- Jackson, B., Arras, P., Penev, K., Peacock, S., & Marchant, P. 2017, *ApJ*, **835**, 145
- Jackson, B., Barnes, R., & Greenberg, R. 2009, *ApJ*, **698**, 1357
- Jackson, B., Greenberg, R., & Barnes, R. 2008, *ApJ*, **678**, 1396
- James, D. J., Barnes, S. A., Meibom, S., et al. 2010, *A&A*, **515**, A100
- Kalirai, J. S., Fahlman, G. G., Richer, H. B., & Ventura, P. 2003, *AJ*, **126**, 1402
- Kearns, K. E., Eaton, N. L., Herbst, W., & Mazzurco, C. J. 1997, *AJ*, **114**, 1098
- Lanza, A. F. 2010, *A&A*, **512**, A77
- Lanza, A. F., & Shkolnik, E. L. 2014, *MNRAS*, **443**, 1451
- Leiner, E. M., Mathieu, R. D., Gosnell, N. M., & Geller, A. M. 2015, *AJ*, **150**, 10
- Li, G., Naoz, S., Kocsis, B., & Loeb, A. 2014, *ApJ*, **785**, 116
- Lissauer, J. J., Ragozzine, D., Fabrycky, D. C., et al. 2011, *ApJS*, **197**, 8
- MacLeod, M., Cantiello, M., & Soares-Furtado, M. 2018, *ApJL*, **853**, L1
- Mamajek, E. E., & Hillenbrand, L. A. 2008, *ApJ*, **687**, 1264
- McQuillan, A., Aigrain, S., & Mazeh, T. 2013, *MNRAS*, **432**, 1203
- Meibom, S., Mathieu, R. D., & Stassun, K. G. 2009, *ApJ*, **695**, 679
- Meibom, S., Mathieu, R. D., Stassun, K. G., Liebesny, P., & Saar, S. H. 2011, *ApJ*, **733**, 115
- Mestel, L. 1968, *MNRAS*, **138**, 359
- Metzger, B. D., Giannios, D., & Spiegel, D. S. 2012, *MNRAS*, **425**, 2778
- Metzger, B. D., Shen, K. J., & Stone, N. 2017, *MNRAS*, **468**, 4399
- Moraux, E., Artemenko, S., Bouvier, J., et al. 2013, *A&A*, **560**, A13
- Muñoz, D. J., & Lai, D. 2015, *PNAS*, **112**, 9264
- Naoz, S. 2016, *ARA&A*, **54**, 441
- Naoz, S., & Fabrycky, D. C. 2014, *ApJ*, **793**, 137
- Naoz, S., Farr, W. M., Lithwick, Y., Rasio, F. A., & Teysandier, J. 2011, *Nature*, **473**, 187
- Naoz, S., Farr, W. M., Lithwick, Y., Rasio, F. A., & Teysandier, J. 2013, *MNRAS*, **431**, 2155
- Naoz, S., Farr, W. M., & Rasio, F. A. 2012, *ApJL*, **754**, L36
- Nardiello, D., Bedin, L. R., Nascimbeni, V., et al. 2015, *MNRAS*, **447**, 3536
- Netopil, M., Paunzen, E., Heiter, U., & Soubiran, C. 2016, *A&A*, **585**, A150
- Parker, E. N. 1958, *ApJ*, **128**, 664
- Pejcha, O., Metzger, B. D., & Tomida, K. 2016, *MNRAS*, **455**, 4351
- Petrovich, C. 2015a, *ApJ*, **799**, 27
- Petrovich, C. 2015b, *ApJ*, **808**, 120
- Petrovich, C., & Tremaine, S. 2016, *ApJ*, **829**, 132
- Pizzolato, N., Maggio, A., Micela, G., Sciortino, S., & Ventura, P. 2003, *A&A*, **397**, 147
- Pollack, J. B., Hubickyj, O., Bodenheimer, P., et al. 1996, *Icar*, **124**, 62
- Quillen, A. C. 2002, *AJ*, **124**, 400
- Raghavan, D., McAlister, H. A., Henry, T. J., et al. 2010, *ApJS*, **190**, 1
- Rasio, F. A., & Ford, E. B. 1996, *Sci*, **274**, 954
- Reimers, D., & Koester, D. 1988, *A&A*, **202**, 77
- Rice, K. 2015, *MNRAS*, **448**, 1729
- Saar, S. H., & Brandenburg, A. 1999, *ApJ*, **524**, 295
- Sarrazine, A. R., Steinhauer, A. J. B., Deliyannis, C. P., et al. 2000, *BAAS*, **32**, 742
- Schatzman, E. 1962, *AnAp*, **25**, 18
- Schuler, S. C., King, J. R., Fischer, D. A., Soderblom, D. R., & Jones, B. F. 2003, *AJ*, **125**, 2085
- Sekiguchi, M., & Fukugita, M. 2000, *AJ*, **120**, 1072
- Soderblom, D. R., Laskar, T., Valenti, J. A., Stauffer, J. R., & Rebull, L. M. 2009, *AJ*, **138**, 1292
- Somers, G., & Stassun, K. G. 2017, *AJ*, **153**, 101
- Stephan, A. P., Naoz, S., & Gaudi, B. S. 2018, *AJ*, in press (arXiv:1806.04145)
- Stephan, A. P., Naoz, S., & Zuckerman, B. 2017, *ApJL*, **844**, L16
- Storch, N. I., & Lai, D. 2015, *MNRAS*, **448**, 1821

- Teitler, S., & Königl, A. 2014, [ApJ](#), **786**, 139
- Tutukov, A. V., & Fedorova, A. V. 2012, [ARep](#), **56**, 305
- Valsecchi, F., & Rasio, F. A. 2014, [ApJL](#), **787**, L9
- van Saders, J. L., Ceillier, T., Metcalfe, T. S., et al. 2016, [Natur](#), **529**, 181
- van Saders, J. L., & Pinsonneault, M. H. 2013, [ApJ](#), **776**, 67
- von Hippel, T., Steinhauer, A., Sarajedini, A., & Deliyannis, C. P. 2002, [AJ](#), **124**, 1555
- Weber, E. J., & Davis, L., Jr. 1967, [ApJ](#), **148**, 217
- Weiss, L. M., & Marcy, G. W. 2014, [ApJL](#), **783**, L6
- Wright, J. T., Marcy, G. W., Howard, A. W., et al. 2012, [ApJ](#), **753**, 160